



## A concise synthesis of Se/Fe materials for catalytic oxidation reactions of anthracene and polyene



Xiaoxue Li<sup>a</sup>, Hongwei Zhou<sup>b</sup>, Rongrong Qian<sup>c</sup>, Xu Zhang<sup>a,\*</sup>, Lei Yu<sup>a,\*</sup>

<sup>a</sup> School of Chemistry and Chemical Engineering, Yangzhou University, Yangzhou 225002, China

<sup>b</sup> College of Biological, Chemical Sciences and Engineering, Jiaxing University, Jiaxing 314001, China

<sup>c</sup> Jiangsu College of Tourism, Yangzhou 225009, China

### ARTICLE INFO

#### Article history:

Received 19 March 2024

Revised 10 May 2024

Accepted 21 May 2024

Available online 22 May 2024

#### Keywords:

Selenium  
Anthracene  
Polyene  
Oxidation  
Deoxygenation

### ABSTRACT

The synergistic effect of Se with Fe can enhance the catalytic activities of the system for oxidation reactions. Based on this principle, a series of Se/Fe materials have been invented to develop the heterogeneous catalysts with industrial application potential. However, the present methods suffer from the tedious procedures, the high reaction temperature, and the low synthetic efficiency. In this paper, we report the synthesis of Se/Fe materials just by precipitating  $\text{Fe}(\text{NO}_3)_3$  with the in situ prepared aqueous  $\text{NaSe}/\text{NaSeO}_3$  under mild conditions. The concise method may resolve the issues hindering the large-scale applications of Se/Fe materials.

© 2025 Published by Elsevier B.V. on behalf of Chinese Chemical Society and Institute of Materia Medica, Chinese Academy of Medical Sciences.

Selenium (Se) is a unique chalcogen element with broad application scopes [1–7]. The atomic radius of Se is larger than sulphur (S), resulting in the weaker binding force to its outer electrons. Thus, Se is more easily oxidized than S. Comparatively, the hybrid orbital and bond length of  $\text{Se}=\text{O}$  are longer than that of  $\text{S}=\text{O}$ , resulting in the weaker  $\pi$  bonds that can be easily reduced [8]. The above features make Se to be a good oxygen carrier that can be employed as the catalyst for oxidation reactions [9]. In 2019, we found that, introducing iron salts into the organoselenium catalyst system could significantly enhance its activity for oxidative deoxygenation reactions, as being reflected by the fact that molecular oxygen could be employed as the oxidant in the presence of the  $\text{PhCH}_2\text{Se}(\text{O})\text{OH}/\text{FeSO}_4$  bi-component catalytic system [10]. In the reaction, Se catalysed the oxidative deoxygenation reaction, while Fe facilitates the activation of molecular oxygen, *i.e.*, catalysed by Fe, the aerobic oxidation of low valent Se to the active  $\text{Se}=\text{O}$  could be achieved, resulting in the less consumption of chemical oxidants such as  $\text{H}_2\text{O}_2$ . Later, a series of bi-component Se/metal catalysts have been developed such as the Se/Cu [11], Se/Ag [12], Se/Mn [13], and Se/Al [14].

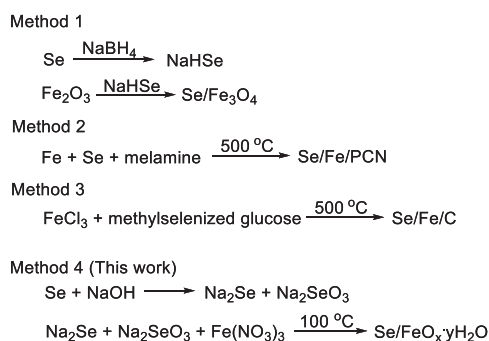
On the other hand, heterogeneous catalysts are practical for large-scale applications [15–19], while using iron as catalyst component is also preferable for the low cost of the metal [20–25]. Thus, developing heterogeneous Se/Fe catalysts may be a good

research topic with industrial application potential. However, the present technologies for preparing Se/Fe materials are not practical. For example, Se/Fe materials could be fabricated *via* the nucleophilic addition at  $\text{Fe}_2\text{O}_3$  with  $\text{NaHSe}$ , which was generated *in situ* by the reduction of Se powder with  $\text{NaBH}_4$  (Scheme 1, Method 1) [26]. The process may release  $\text{H}_2\text{Se}$ , which is a toxic gas hazardous to the environments. Moreover,  $\text{H}_2$  gas is also generated during the reaction, and it must be carefully treated to avoid explosion accident in large-scale production [27]. Another method for preparing Se/Fe catalyst is by calcining the Se and Fe powders with melamine, but it requires high calcination temperature at  $500^\circ\text{C}$  and most of the weight of melamine lost during the process (Scheme 1, Method 2) [28]. Se/Fe material can be prepared by calcining methylselenized glucose [29] with  $\text{FeCl}_3$  [30]. However, despite the high calcining temperature ( $500^\circ\text{C}$ ), the expensive price of methylselenized glucose may bottleneck the application of the method in industry (Scheme 1, Method 3). Recently, we developed a new concise method to fabricate Se/Fe materials more efficiently (Scheme 1, Method 4). Herein, we wish to report our findings.

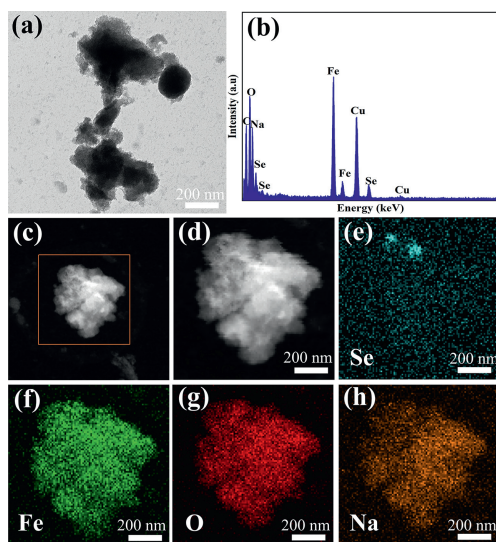
The material was fabricated *via* the co-precipitation of iron salt with selenium species under alkaline conditions. Heating selenium powder with aqueous  $\text{NaOH}$  initially led to the mixture of  $\text{Na}_2\text{Se}$  and  $\text{Na}_2\text{SeO}_3$  *via* the disproportionated reaction of  $\text{Se}^0$  to  $\text{Se}^{2-}$  and  $\text{Se}^{4+}$  (Scheme 1, Method 4). After cooling to room temperature, aqueous  $\text{Fe}(\text{NO}_3)_3$  was added to precipitate selenium. The precipitations were dried at  $100^\circ\text{C}$  in a simple bake out furnace just in

\* Corresponding authors.

E-mail addresses: [zhangxu@yzu.edu.cn](mailto:zhangxu@yzu.edu.cn) (X. Zhang), [yulei@yzu.edu.cn](mailto:yulei@yzu.edu.cn) (L. Yu).



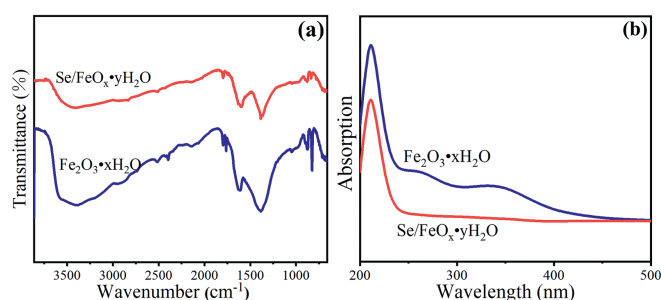
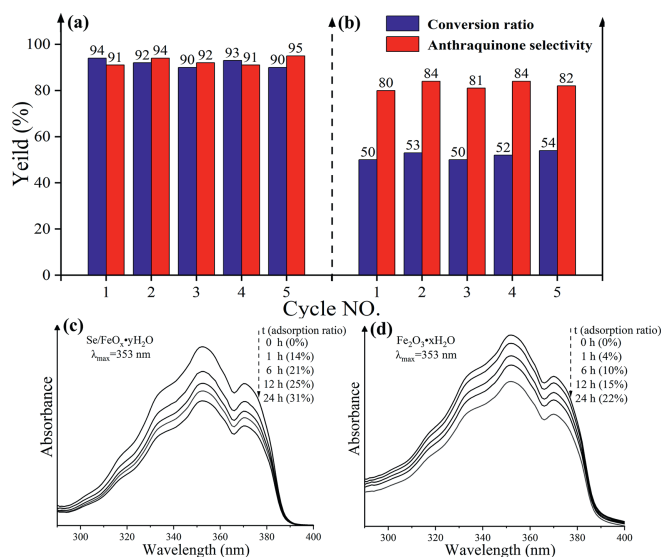
Scheme 1. Comparison of the methods.

Fig. 1. Composition analysis of Se/FeO<sub>x</sub>·yH<sub>2</sub>O.

open air to afford the iron oxide-supported selenium marked as Se/FeO<sub>x</sub>·yH<sub>2</sub>O.

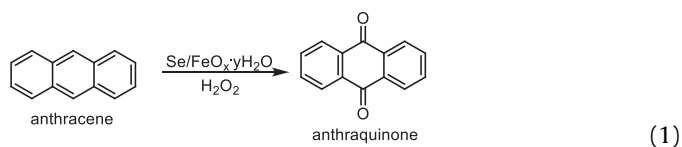
Transmission electron microscopy (TEM) image shows that selenium dispersed uniformly on the surface of the material, and it may be in amorphous state (Fig. 1a). Energy dispersive X-ray spectroscopy (EDX) confirmed the successful loading of selenium onto the iron oxide support (Fig. 1b). High angle annular dark field scanning electron microscopy (HAADF-STEM) and element mapping images can effectively reflect the composition and dispersion of the elements in the material. HAADF-STEM images are highly sensitive to changes in atomic number of atoms in the sample (Z-contrast images). Specifically, the contrast intensity of Z is directly proportional to the square of the atomic number [31]. Therefore, the bright area may be attributed to the Se element in the HAADF-STEM image of Se/FeO<sub>x</sub>·yH<sub>2</sub>O (Figs. 1c and d). The element mapping images in Figs. 1e–h reflect the uniform dispersion of Se, Fe, O, and Na elements. Dispersive distribution of Se indicates that the element may also be involved by physical adsorption (Fig. 1e).

Fourier-transform infrared (FT-IR) and ultraviolet-visible (UV-vis) analyses of the materials were then conducted to get the information of the functional groups in the materials. Unselenized Fe<sub>2</sub>O<sub>3</sub>·xH<sub>2</sub>O was prepared in similar method and analysed for comparison. The IR spectra of Se/FeO<sub>x</sub>·yH<sub>2</sub>O and Fe<sub>2</sub>O<sub>3</sub>·xH<sub>2</sub>O were generally the same, and no additional peak emerged. This indicates that the selenium content in the material was particularly low, and the formed selenium-containing bonds were difficult to be observed in its IR spectrum (Fig. 2a). This conclusion was then verified by the inductively coupled plasma mass spectroscopy (ICP-MS)

Fig. 2. IR (a) and UV-vis (b) spectra of Fe<sub>2</sub>O<sub>3</sub>·xH<sub>2</sub>O and Se/FeO<sub>x</sub>·yH<sub>2</sub>O.Fig. 3. Studies on the materials: (a) Recycling and reusing of Se/FeO<sub>x</sub>·yH<sub>2</sub>O. (b) Recycling and reusing of Fe<sub>2</sub>O<sub>3</sub>·xH<sub>2</sub>O. Adsorption of anthracene on Se/FeO<sub>x</sub>·yH<sub>2</sub>O (c) and Fe<sub>2</sub>O<sub>3</sub>·xH<sub>2</sub>O (d).

analysis of the material, which verified that selenium content in Se/FeO<sub>x</sub>·yH<sub>2</sub>O was only 3.5%. IR spectra indicated that the water-content of Fe<sub>2</sub>O<sub>3</sub>·xH<sub>2</sub>O was higher than that of Se/FeO<sub>x</sub>·yH<sub>2</sub>O, as being reflected by the even stronger signals at ca. 3500 cm<sup>-1</sup>. The influence of water content was more significant in UV-vis spectra, and it caused the red-shift in the spectrum and led to the peaks at 250–350 nm (Fig. 2b).

As a material containing both selenium and iron, Se/FeO<sub>x</sub>·yH<sub>2</sub>O was supposed to be a nice catalyst for oxidation reactions. Its catalytic activity was initially evaluated via the oxidation reaction of anthracene to anthraquinone (Eq. 1). Anthracene is a pollutant that was abundantly produced from coal chemical industry, while anthraquinone is now a basic raw material for the synthesis of organic light-emitting materials (OLEMs), which are electronic chemicals of profound market prospect [32–34]. Thus, the reaction is a significant industrial process and deserves investigations.



As shown in Fig. 3a, catalysed by Se/FeO<sub>x</sub>·yH<sub>2</sub>O, the oxidation of anthracene occurred smoothly and produced the desired anthraquinone in good yields. As a heterogeneous catalyst with magnetic features, Se/FeO<sub>x</sub>·yH<sub>2</sub>O could be removed from the mixture by magnetic separation after reaction. It is reusable, and the recy-

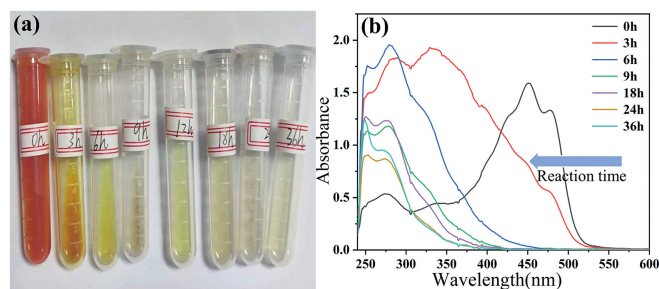


Fig. 4. (a) Photographs and (b) UV-vis spectra of the samples of  $\beta$ -carotene degradation reactions with  $\text{Se/FeO}_x \cdot y\text{H}_2\text{O}$ .

clad catalyst could be directly reused without deactivation. In the reactions, both the conversion ratio of anthracene and the selectivity of anthraquinone were over 90%, showing sufficient utilization of the atoms in starting materials from the industrial viewpoint (Fig. 3a). The catalytic activity of unselenized  $\text{Fe}_2\text{O}_3 \cdot x\text{H}_2\text{O}$  was also tested for comparison, but led to poor anthracene conversion, and the selectivity of anthraquinone also decreased (Fig. 3b). Thus, it may be concluded that the oxygen-carrier properties of selenium endow the material good catalytic activity for oxidation reactions, which has been well summarized by literatures [35–40].

It has been reported that selenization may change the surface properties of the materials and affect the mass-transfer processes during the catalytic reactions [41,42]. Thus, the elevated catalytic activity of  $\text{Se/FeO}_x \cdot y\text{H}_2\text{O}$  versus unselenized  $\text{Fe}_2\text{O}_3 \cdot x\text{H}_2\text{O}$  may also attribute to the improved mass-transfer properties of the materials. To verify or exclude this possibility, anthracene adsorption experiments were performed with  $\text{Se/FeO}_x \cdot y\text{H}_2\text{O}$  and  $\text{Fe}_2\text{O}_3 \cdot x\text{H}_2\text{O}$ . As shown in Fig. 3c, ca. 31% of anthracene was adsorbed on  $\text{Se/FeO}_x \cdot y\text{H}_2\text{O}$  after 24 h immersing, but for  $\text{Fe}_2\text{O}_3 \cdot x\text{H}_2\text{O}$ , this value was only 22% after the same time immersing (Fig. 3d). The result clearly demonstrated that the mass-transfer process on  $\text{Se/FeO}_x \cdot y\text{H}_2\text{O}$  was better than the unselenized  $\text{Fe}_2\text{O}_3 \cdot x\text{H}_2\text{O}$ .

On the other hand, polyenes are common pollutants in pharmaceutical industry [43,44], and they may be treated by the oxidative degradation splitting the C=C bond. Our recent investigations have demonstrated that the oxidative C=C cleavage reaction could be catalysed by selenium, while iron significantly promoted the catalytic activity [45,46]. Thus, as a heterogeneous catalyst containing both selenium and iron,  $\text{Se/FeO}_x \cdot y\text{H}_2\text{O}$  may be applied in polyene degradation reaction. In this work, we chose the degradation of  $\beta$ -carotene as the model reaction to evaluate the catalytic activity of  $\text{Se/FeO}_x \cdot y\text{H}_2\text{O}$ . As shown in Fig. 4a, the colour of  $\beta$ -carotene faded smoothly during the process. Moreover, UV-vis spectra in Fig. 4b clearly indicated the blue shift of the samples along with the reaction time, reflecting the C=C bond cleavage leading to the colourless small molecules. Mass-spectra of the reaction mixtures (Figs. S2–S5 in Supporting information) could verify that the  $\text{Se/FeO}_x \cdot y\text{H}_2\text{O}$ -catalyzed oxidation reaction of  $\beta$ -carotene could result in the C=C bond splitting leading to produce a variety of fragments such as the  $\beta$ -ionone.

X-ray photoelectron spectroscopy (XPS) analysis was then conducted to evaluate the stability of the catalysts during the reaction processes. In the XPS spectra, the signals of Se  $3d_{5/2}$  and Se  $3d_{3/2}$  of fresh  $\text{Se/FeO}_x \cdot y\text{H}_2\text{O}$  emerged at 55.8 and 56.8 eV respectively. They did not change much after the five times reaction (Fig. 3a), showing that the valence of selenium was stable during the catalytic oxidation reaction process (Fig. 5a). In the Fe 2p spectra, signals at 711.5 and 725.1 eV reflected Fe  $2p_{3/2}$  and Fe  $2p_{1/2}$  respectively, and their compositions were generally stable during the reaction process (Fig. 5b). There were only  $\text{Se}^{4+}$  and  $\text{Se}^{2+}$  species in the material, while the  $\text{Se}^{2-}$  species disappeared. For iron, both

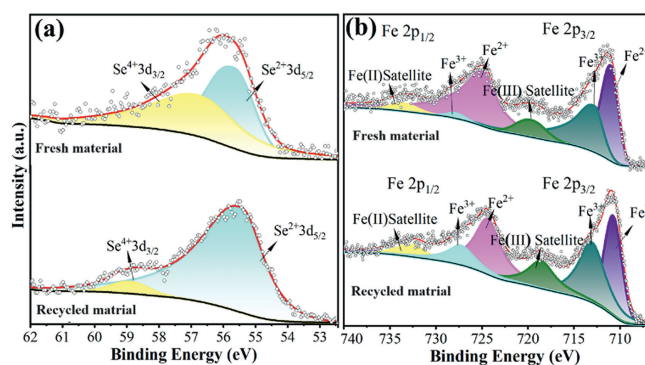


Fig. 5. XPS analysis of  $\text{Se/FeO}_x$ .

$\text{Fe}^{2+}$  and  $\text{Fe}^{3+}$  species were observed in XPS spectra. This phenomenon demonstrated that the redox reaction occurred between the disproportionated reaction-generated reductive  $\text{Se}^{2-}$  and the oxidative  $\text{Fe}^{3+}$ . The O 1s spectra of the materials (Fig. S1 in Supporting information) indicated there were three kinds of oxygen, such as  $\text{O}_L$ ,  $\text{O}_V$  and the hydroxyl oxygen, and the strength of the signals were determined by the concentration of the oxygen vacancy. The content of hydroxyl oxygen decreased obviously after reaction, reflecting the aging process releasing water from the material.

In conclusion, we have reported a new method for preparing Se/Fe materials concisely. It was found that, just by heating Se with NaOH could lead to the water soluble selenium salts such as  $\text{Na}_2\text{Se}$  and  $\text{Na}_2\text{SeO}_3$ , which were precipitated by  $\text{Fe}(\text{NO}_3)_3$  and led to  $\text{Se/FeO}_x \cdot y\text{H}_2\text{O}$  after simple drying at  $100^\circ\text{C}$ . The material could catalyse the selective oxidation of anthracene to produce anthraquinone, a basic material of OLEM industry. It is also applicable for polyene degradation. Indeed, the purpose of this work is not only limited on the synthesis of anthraquinone or the degradation of polyene. It proposes a new approach for the rapid synthesis of selenium containing materials, which will have a profound impact in the field of selenium science and materials and industry.

#### Declaration of competing interest

The authors declare that they have no known competing financial interests or personal relationships that could have appeared to influence the work reported in this paper.

#### CRediT authorship contribution statement

**Xiaoxue Li:** Writing – original draft, Investigation. **Hongwei Zhou:** Writing – review & editing, Supervision. **Rongrong Qian:** Writing – original draft. **Xu Zhang:** Supervision, Investigation. **Lei Yu:** Writing – review & editing, Supervision, Project administration, Conceptualization.

#### Acknowledgments

We thank the Jiangsu Provincial Six Talent Peaks Project (No. XCL-090), the Cooperation Project of Yangzhou City with Yangzhou University (No. YZ2023209), Jiaying Key Laboratory for Creation of Animal Models & Synthesis of Lead Compounds of New Drug (No. jxsx21006), and the Priority Academic Program Development of Jiangsu Higher Education Institutions for support.

#### Supplementary materials

Supplementary material associated with this article can be found, in the online version, at doi:10.1016/j.ccl.2024.110036.

## References

- [1] D. Yong, J. Tian, R. Yang, Q. Wu, X. Zhang, *Chin. J. Org. Chem.* 44 (2024) 1343–1347.
- [2] J. Li, Q. Shi, Y. Xue, et al., *Chin. Chem. Lett.* 35 (2024) 109239.
- [3] L. Xian, Q. Li, T. Li, L. Yu, *Chin. Chem. Lett.* 34 (2023) 107878.
- [4] W. Ding, S. Wang, J. Gu, L. Yu, *Chin. Chem. Lett.* 34 (2023) 108043.
- [5] J. Zhou, X. Xu, H. Wu, et al., *Nat. Energy* 8 (2023) 526–535.
- [6] Z. Zhao, S. Laps, J.S. Gichtin, N. Metanis, *Nat. Rev. Chem.* 8 (2024) 211–229.
- [7] Z. Wang, X. Wang, Q. Li, et al., *Chin. Chem. Lett.* 35 (2024) 109058.
- [8] W. Hou, H. Xu, *J. Med. Chem.* 65 (2022) 4436–4456.
- [9] A.J. Pacuła-Miszewska, L. Sancineto, Oxygen-transfer reactions catalyzed by organoselenium compounds, in: E.J. Lenardão, C. Santi, G. Perin, D. Alves (Eds.), *Organochalcogen Compounds*, Elsevier, 2022, pp. 219–249.
- [10] C. Chen, X. Zhang, H. Cao, et al., *Adv. Synth. Catal.* 361 (2019) 603–610.
- [11] C. Chen, Z. Cao, X. Zhang, et al., *Chin. J. Chem.* 38 (2020) 1045–1051.
- [12] F. Liu, J. Zhan, Y. Sun, X. Jing, *Chin. J. Org. Chem.* 41 (2021) 2099–2104.
- [13] Y. Zeng, T. Chen, X. Zhang, et al., *Appl. Organomet. Chem.* 36 (2022) e6658.
- [14] X. Zhang, R. Zhou, Z. Qi, et al., *React. Chem. Eng.* 7 (2022) 1990–1996.
- [15] R.N. Yi, W.M. He, *Chin. Chem. Lett.* 35 (2024) 109253.
- [16] F.L. Zeng, H.L. Zhu, R.N. Wang, et al., *Chin. J. Catal.* 46 (2023) 157–166.
- [17] Y.H. Lu, C. Wu, J.C. Hou, et al., *ACS Catal.* 13 (2023) 13071–13076.
- [18] H.Y. Song, J. Jiang, C. Wu, et al., *Green Chem.* 25 (2023) 3292–3296.
- [19] W.T. Ouyang, H.T. Ji, J. Jiang, et al., *Chem. Commun.* 59 (2023) 14029–14032.
- [20] G. Zhang, C. Zhang, Y. Tian, F. Chen, *Org. Lett.* 25 (2023) 917–922.
- [21] H. Zhang, T. Yang, H. Zhou, et al., *Appl. Catal. B* 342 (2024) 123391.
- [22] H. Sun, J. Wu, F. Tian, et al., *Catal. Sci. Technol.* 14 (2024) 660–666.
- [23] Z. Han, Y. Zhu, X. Yao, et al., *Appl. Catal. B* 337 (2023) 122961.
- [24] C. Pei, Y. Gu, Z. Liu, X. Yu, L. Feng, *ChemSusChem* 12 (2019) 3849–3855.
- [25] Y. Li, L. Zhang, Z. Zhang, et al., *Adv. Synth. Catal.* 358 (2016) 2148–2155.
- [26] X. Chen, J. Mao, C. Liu, et al., *Chin. Chem. Lett.* 31 (2020) 3205–3208.
- [27] W. Zhou, P. Li, J. Liu, L. Yu, *Ind. Eng. Chem. Res.* 59 (2020) 10763–10767.
- [28] W. Zhou, X. Xiao, Y. Liu, X. Zhang, *Chin. J. Org. Chem.* 42 (2022) 1849–1855.
- [29] Q. Wang, P. Li, T. Li, et al., *Ind. Eng. Chem. Res.* 60 (2021) 8659–8663.
- [30] H. Cao, P. Li, X. Jing, H. Zhou, *Chin. J. Org. Chem.* 42 (2022) 3890–3895.
- [31] K. Sohlberg, T.J. Pennycook, W. Zhou, S.J. Pennycook, *Phys. Chem. Chem. Phys.* 17 (2015) 398–406.
- [32] Y. Liu, Z. Li, Y. Xu, et al., *ACS Appl. Mater. Interfaces* 16 (2024) 9436–9442.
- [33] N.N. Ayare, P.O. Gupta, M.C. Sreenath, et al., *Spectrochim. Acta A* 246 (2021) 119017.
- [34] L. Chen, Y. Chen, H. Fu, et al., *Adv. Sci.* 7 (2020) 2000803.
- [35] J.T. Stadel, T.G. Back, *Chem. Eur. J.* 30 (2024) e202304074.
- [36] S. Dyjak, B.J. Jankiewicz, S. Kaniecki, W. Kiciński, *Green Chem.* 26 (2024) 2985–3020.
- [37] X. Xiao, C. Guan, J. Xu, W. Fu, L. Yu, *Green Chem.* 23 (2021) 4647–4655.
- [38] H. Cao, R. Qian, L. Yu, *Catal. Sci. Technol.* 10 (2020) 3113–3121.
- [39] F.V. Singh, T. Wirth, *Catal. Sci. Technol.* 9 (2019) 1073–1091.
- [40] L. Shao, Y. Li, J. Lu, X. Jiang, *Org. Chem. Front.* 6 (2019) 2999–3041.
- [41] K. Cao, X. Deng, T. Chen, Q. Zhang, L. Yu, *J. Mater. Chem. A* 7 (2019) 10918–10923.
- [42] P. Li, Z. Qi, L. Yu, H. Zhou, *Catal. Sci. Technol.* 12 (2022) 2241–2247.
- [43] S.K. Alharbi, W.E. Price, *Curr. Pollut. Rep.* 3 (2017) 268–280.
- [44] Y. Miao, Y. Zhao, G. Waterhouse, et al., *Nat. Commun.* 14 (2023) 4242.
- [45] X. Li, H. Hua, Y. Liu, L. Yu, *Org. Lett.* 25 (2023) 6720–6724.
- [46] T. Wang, X. Jing, C. Chen, L. Yu, *J. Org. Chem.* 82 (2017) 9342–9349.